



OPEN Interactive effects of diurnal temperature range and air pollution on myocardial infarction incidence: an individual-level case-crossover study

Xi-yun Gong^{1,4}, Zai-chao Dong^{2,4}, Tong-tong Sha², Qian Li², Yan-jie Dou², Huan-xia Zhang², Yao Li², Hai-tao Wei³✉ & Fang-fang Yu²✉

Climate change and air pollution have garnered increasing attention in recent years due to their potential to contribute to various diseases, including myocardial infarction (MI). However, no previous studies have explored the interactive effects of diurnal temperature range (DTR) and air pollution on MI. This study employed an individual-level time-stratified case-crossover design to investigate 391,901 MI patients in central China between 2017 and 2020. Daily estimated air pollutant concentrations for each patient were extracted from gridded datasets based on their residential addresses on both case and control days. Conditional logistic regression models were used to examine the lagged effects and exposure-response relationships between short-term exposure to air pollutants, DTR, and MI. Additionally, the relative excess odds due to interaction (REOI), proportion attributable to interaction, and synergy index were applied to quantify the interaction effects. Subgroup analyses were further conducted by gender and age (≥ 65 years old and < 65 years old) to identify vulnerable populations. Exposure to all six air pollutants (PM_{2.5}, PM₁₀, SO₂, NO₂, CO, O₃) was significantly associated with an elevated risk of MI. The risks of PM_{2.5}, PM₁₀, SO₂, and CO became more pronounced after exceeding specific threshold concentrations. For O₃ exposure, MI risk was reduced when concentrations were below the critical threshold but increased when this threshold was exceeded. High DTR was independently associated with an increased MI risk. Significant antagonistic interactions between air pollutant exposure and high DTR were observed across multiple lag periods. This study reveals that the adverse effects of air pollutants on MI are attenuated under high DTR conditions, highlighting the complex interplay between DTR and air pollution in the pathogenesis of MI.

Keywords Diurnal temperature range, Air pollution, Myocardial infarction, Interactive effects

As the fundamental component of the natural environment and resources underpinning human survival, environmental and climatic factors are intricately linked to living conditions and social activities¹. In recent decades, direct and indirect impacts on human health have been exerted by climate change, triggering frequent, intense, and widespread extreme weather events (cold waves, heatwaves, and dramatic temperature fluctuations), which pose significant risks to public health systems and emergency medical services². Numerous studies have demonstrated that extreme temperatures can induce various diseases, which alter disease incidence and mortality risks^{3–5}. While daily mean temperature has been widely used as an evaluation metric by most research^{6,7}, this measure may inadequately capture the severity of temperature fluctuations during periods of significant variation⁸. Diurnal temperature range (DTR) serves as a critical indicator of short-term temperature variation, quantifying intraday temperature dynamics⁹. Early investigations have highlighted

¹Department of Emergency Medicine, The First Affiliated Hospital of Zhengzhou University, Zhengzhou 450052, China. ²Department of Environmental Health, School of Public Health, Zhengzhou University, 100 Kexue Avenue, Zhengzhou 450001, Henan, China. ³The school of the Geo-Science & Technology, Zhengzhou University, 100 Kexue Avenue, Zhengzhou 450000, Henan, China. ⁴Xi-yun Gong and Zai-chao Dong contributed equally as co-first authors. ✉email: zzu_wei@zzu.edu.cn; yufangfang@zzu.edu.cn

associations between DTR and the incidence/mortality of cardiovascular, cerebrovascular, and respiratory diseases^{10,11}, yet their relationship with myocardial infarction (MI) risk remains poorly characterized.

MI is a life-threatening condition caused by acute coronary artery occlusion leading to myocardial ischemia and necrosis, it is represented as a leading cause of global cardiovascular morbidity and mortality^{12,13}, accounting for > 30% of ischemic heart disease deaths¹⁴. MI may be triggered by rapid temperature shifts through multiple pathways, including alterations in heart rate and blood viscosity, induction of systemic inflammation, immune suppression, and disruption of thermoregulatory mechanisms¹¹. Air pollution is represented as a leading environmental risk factor for global mortality and disease burden¹⁵, and primarily consists of particulate matter and gaseous pollutants. Particulate matter includes fine particulate matter (PM_{2.5}) and inhalable particulate matter (PM₁₀), while gaseous pollutants comprise sulfur dioxide (SO₂), nitrogen dioxide (NO₂), carbon monoxide (CO), and ozone (O₃). Substantial evidence confirmed that short-term exposure to air pollutants markedly elevates MI risk¹⁶, with co-exposure to PM_{2.5} and heatwaves demonstrating synergistic effects on MI mortality¹⁷. Despite established interactions between heatwaves and PM_{2.5}, the combined impact of DTR and air pollution on MI risk remains unknown, with an issue of critical significance amid escalating climate variability.

To address this critical issue, we conducted an individual-level case-crossover study involving 391,901 MI patients in Henan Province, China (2017–2020). This research aims to: (1) evaluate associations between extreme DTR, air pollutants, and MI risk; (2) quantify interaction effects between DTR and air pollution; and (3) identify potential susceptible populations.

Methods

Study area

This study was conducted in Henan Province, China (31°23′–36°22′N, 110°21′–116°39′E), situated in central China along the middle-lower Yellow River basin (Fig. 1A). By the end of 2020, the province had a permanent population of 99.41 million, with 55.43% urban residents, 50.1% male population, and 13.5% aged over 65 years old.

Geographically, most of Henan lies in the warm temperate zone, with its southern region spanning the subtropical zone, characterized by a continental monsoon climate. The terrain transitions from plains to hilly mountains from east to west, featuring distinct seasons, concurrent rainfall and heat, and frequent climatic disasters (<https://slt.henan.gov.cn/>; accessed 26 June 2025). The Henan province has an annual average temperature of 12–16 °C, annual precipitation of 400–1100 mm, and annual sunshine hours of 1500–2200 h.

Air pollutant and meteorological data

Air pollution data were obtained from the China High Air Pollutants (CHAP) dataset, comprising daily measurements of six major pollutants (PM_{2.5}, PM₁₀, SO₂, NO₂, CO, and O₃) in Henan Province from 1 January 2017 to 31 December 2020¹⁸. Specifically, the PM_{2.5}, PM₁₀, SO₂, NO₂, and CO data represented 24-hour average concentrations, while O₃ data denoted daily maximum 8-hour moving average concentrations. Generated using artificial intelligence, ground-based observations, atmospheric reanalysis, and satellite remote sensing, this high-resolution dataset ensures full coverage of China. The spatial resolution was 1 km for PM_{2.5}, PM₁₀, and O₃; for SO₂, NO₂, and CO, it was 10 km during 2017–2018 year and improved to 1 km (higher precision) during 2019–2020 year. Validation against ground monitoring stations showed strong consistency: cross-validation coefficients of determination (R²) for PM_{2.5}, PM₁₀, SO₂, NO₂, CO, and O₃ ranged from 0.80 to 0.93, with corresponding root mean square errors (RMSE) of 10.76 µg/m³, 21.12 µg/m³, 10.07 µg/m³, 7.99 µg/m³, 0.29 mg/m³, and 15.77 µg/m³, respectively.

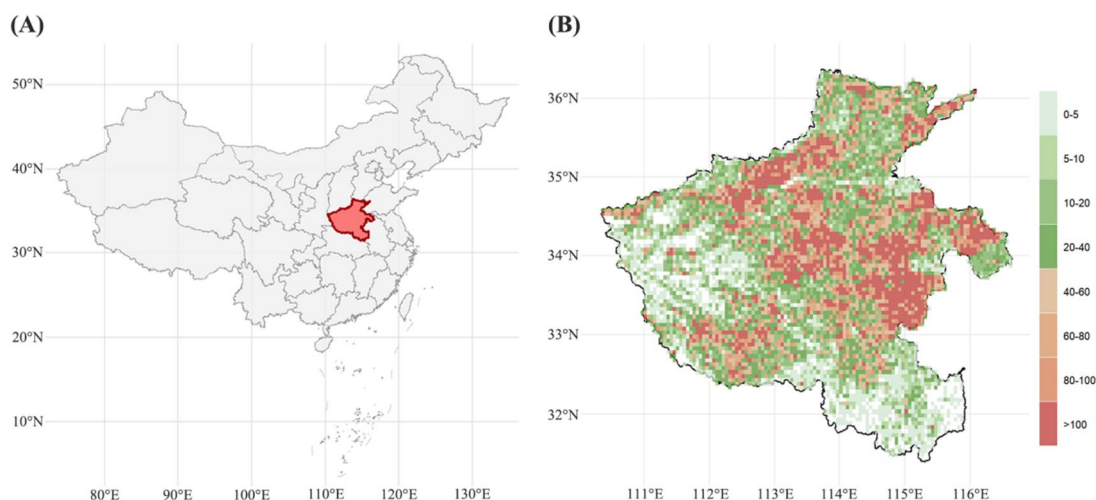


Fig. 1. Spatial distribution of MI cases in Henan province from 2017 to 2020. Location of Henan province in China (A), spatial distribution of cases (B).

Meteorological data were derived from the European Centre for Medium-Range Weather Forecasts (ECMWF) for Fifth Generation ECMWF Reanalysis (ERA5) with a resolution of $0.1^\circ \times 0.1^\circ$, including daily mean temperature ($^\circ\text{C}$), maximum temperature ($^\circ\text{C}$), minimum temperature ($^\circ\text{C}$), and relative humidity (%). DTR was defined as the difference between daily maximum and minimum temperatures.

Firstly, latitude and longitude coordinates were geocoded from MI patients' home addresses using Baidu Maps, which were matched to gridded air pollution and meteorological datasets to derive individual exposures. Thresholds were defined using the 25th (P25) and 75th (P75) percentiles of daily DTR (2017–2020): high DTR was $\geq P75$, low DTR $\leq P25$, and medium DTR between P25–P75.

Study population

This study collected MI case data from 329 hospitals in Henan Province between January 1, 2017, and December 31, 2020. MI cases were diagnosed according to The International Statistical Classification of Diseases and Related Health Problems 10th Revision (ICD-10), including acute MI (I21) and subsequent MI (I22). Medical records included patient demographics (gender, age, current address), admission date, and primary diagnosis. After excluding patients with incomplete records ($n = 1541$, 0.39%), a total of 391,901 MI patients residing in Henan Province during 2017–2020 were included (Fig. 1B). The study protocol was approved by the Ethics Committee of Zhengzhou University, and informed consent was obtained from all subjects and/or their legal guardians.

Study methods

This study employed a time-stratified case-crossover design based on individual exposure, to investigate interactive effects of DTR and air pollution on MI incidence¹⁹. This approach evaluated exposure patterns before and after the case day, with each case serving as its own control to mitigate potential confounding factors. For each MI case, the onset day was designated as the case day, and control days were defined as the same day of the week in the same year and month but different weeks, thereby controlling for long-term trends, seasonality, and personal confounders (e.g., short-term invariable factors included behavioral patterns, health status, and demographic characteristics). Consequently, this study only adjusted for time-varying factors (e.g., mean temperature and relative humidity). According to this method, each case day was matched with 3–4 control days. For example, if a case occurred on the second Monday of September 2017 (September 11), the onset day served as the case day, and other Mondays in September (September 4, 18, and 25) were selected as control days.

Statistical analysis

This study applied Spearman correlation analysis to assess the associations between air pollutants and meteorological factors. Conditional logistic regression models were employed to evaluate the relationships between temperature variations, air pollution exposure, and MI risk. DTR and air pollutants were incorporated into the model both as categorical variables and natural cubic spline functions, with the degrees of freedom (df) set to 3. Consistent with documented lag effects of air pollutants on MI, we examined both single-day lags (lag0–lag7) and cumulative lag exposures (lag01–lag07). Consistent with previous studies, subsequent analyses primarily used exposure data from the period with the strongest effect as the core indicator^{17,20,21}. Exposure-response curves for each air pollutant were generated, and likelihood ratio tests were used to verify nonlinear associations. In the presence of a nonlinear relationship, piecewise conditional logistic regression was applied to identify potential breakpoints. Thereafter, the percentage change in MI risk (defined as $[\text{odds ratio} - 1] \times 100\%$) and its 95% confidence interval (CI) were reported per 1-unit increase ($10 \mu\text{g}/\text{m}^3$ for PM_{2.5}, PM₁₀, SO₂, NO₂, and O₃; $1 \text{mg}/\text{m}^3$ for CO).

Subsequently, we evaluated the interactive effects between high DTR and air pollutants across different lag periods. Using the median (P50) of each air pollutant as the threshold, pollutants were categorized into low and high exposure levels (Table S1). DTR and air pollution groups were then paired to construct a new variable representing their joint exposure, for which odds ratios (ORs) were calculated for each combination. As an illustrative example, consider PM_{2.5} and high DTR: the four variable levels included medium DTR and low-level PM_{2.5} (level 00), high DTR and low-level PM_{2.5} (level 10), medium DTR and high-level PM_{2.5} (level 01), and high DTR and high-level PM_{2.5} (level 11). Using level 00 (OR₀₀=1) as the reference, the OR values were calculated for levels 10 (OR₁₀), 01 (OR₀₁), and 11 (OR₁₁), from which three interaction metrics were calculated: relative excess odds due to interaction (REOI), attributable proportion of interaction (AP), and synergy index (SI). REOI = OR₁₁ - OR₁₀ - OR₀₁ + 1, quantifying the interaction's contribution to the overall effect. AP = REOI/OR₁₁, representing the interaction's proportion in the total effect. SI = (OR₁₁ - 1)/[(OR₁₀ - 1) + (OR₀₁ - 1)], indicating the ratio of the combined effect to individual effects. The delta method was employed to compute 95% CIs for these indices²². A synergistic effect was indicated by REOI > 0, AP > 0, and SI > 1 (i.e., combined effect exceeding individual effects), whereas REOI < 0, AP < 0, and SI < 1 signified an antagonistic interaction.

To identify potentially susceptible populations, stratified analyses were conducted by sex (male and female), age (< 65 and ≥ 65 years), and season (warm [April to September] vs. cold [October to March]). A two-sample Z test was used to assess the statistical significance of differences in effect estimates across subgroups. To verify the robustness of these results, we conducted two sensitivity analyses. First, we adjusted the patient scope by excluding patients with subsequent MI (ICD-10 code: I22). Second, to eliminate the impact of coronavirus disease 2019 (COVID-19), we restricted the patients' onset time to the period from 2017 to 2019. All analyses were conducted using R (version 4.3.1), with two-sided $P < 0.05$ considered statistically significant.

Characteristic	Count (%)
No. of cases	391,901
Acute MI	345,011 (88.0)
Subsequent MI	46,890 (12.0)
Case days	391,901
Control days	1,331,920
Age (years old)	
< 65	154,477 (39.4)
≥ 65	237,410 (60.6)
Sex	
Male	227,550 (58.1)
Female	164,351 (41.9)
Marriage status	
Married	271,060 (69.2)
Single	120,841 (30.8)
Season	
Spring	111,745 (28.5)
Summer	95,495 (24.4)
Autumn	88,433 (22.6)
Winter	96,228 (24.5)

Table 1. Characteristics of study population in Henan province from 2017 to 2020. *MI* myocardial infarction.

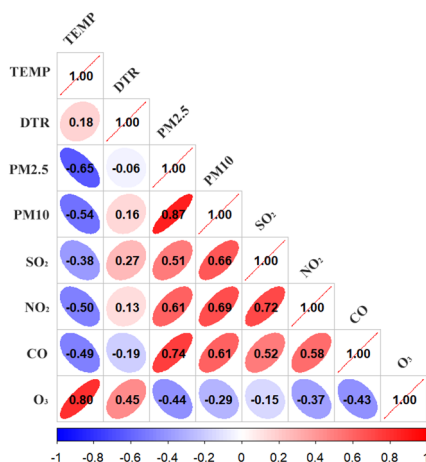


Fig. 2. Spearman's correlation coefficients between environmental factors.

Results

General characteristics

From January 2017 to December 2020, a total of 391,901 MI patients were enrolled, including 345,011 acute MI (88.0%) and 46,890 subsequent MI (12.0%). The study comprised 391,901 case days and 1,331,920 control days. Demographic characteristics showed that 39.4% of patients were aged under 65 years old, 58.1% were male, 69.2% were married, and 28.5% experienced the onset of MI in spring (Table 1).

During the study period, daily mean concentrations of air pollutants were as follows: PM_{2.5} (58.4 $\mu\text{g}/\text{m}^3$), PM₁₀ (101.6 $\mu\text{g}/\text{m}^3$), SO₂ (14.8 $\mu\text{g}/\text{m}^3$), NO₂ (33.7 $\mu\text{g}/\text{m}^3$), CO (1.0 mg/m^3), and O₃ (114.9 $\mu\text{g}/\text{m}^3$). On case days, DTR ranged from 0.3 $^{\circ}\text{C}$ to 23.8 $^{\circ}\text{C}$ (mean: 10.5 $^{\circ}\text{C}$), with daily mean/minimum/maximum temperatures of 15.8 $^{\circ}\text{C}$, 10.4 $^{\circ}\text{C}$, and 20.9 $^{\circ}\text{C}$, respectively (Table S1). Correlation analysis revealed positive associations among PM_{2.5}, PM₁₀, SO₂, NO₂, and CO, while O₃ exhibited negative correlations with other pollutants (Fig. 2). DTR was positively correlated with PM₁₀, SO₂, NO₂, and O₃, and weakly negatively correlated with PM_{2.5} and CO (all $P < 0.05$).

Effects of DTR on the risk of MI

Figure 3 illustrates the effect of each 1 $^{\circ}\text{C}$ increase in DTR on the risk of MI across different lag periods. The results showed that low DTR exerted a protective effect against MI: with an increase in lag days, the impact on MI risk exhibited a decreasing trend, reaching the strongest effect at lag05 [−0.36% (95% CI: −0.59%, −0.13%)].

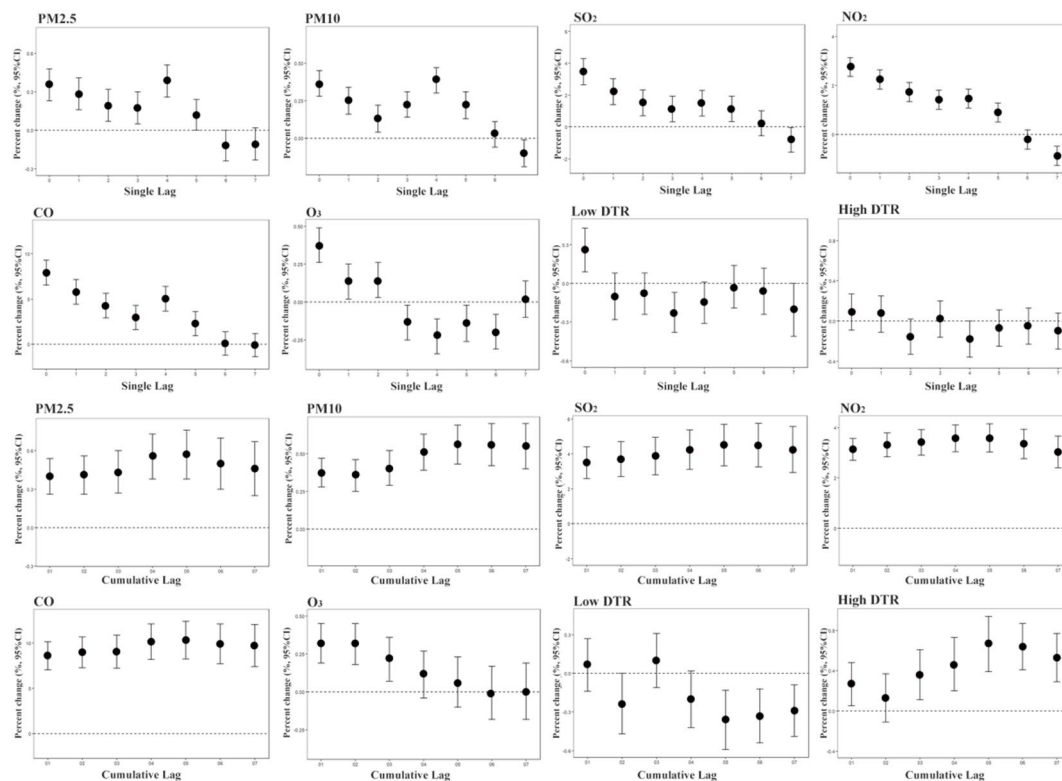


Fig. 3. Lag effect analysis of air pollution and DTR on MI risk, 2017 to 2020.

In contrast, high DTR was associated with an increased risk of MI. As the cumulative lag days increased, the association between high DTR and MI risk exhibited a pattern of first increasing and then decreasing, peaking at lag05 [0.67% (0.39%, 0.94%)]. Therefore, the effect at lag05 was selected as the primary outcome for subsequent analyses.

Effects of air pollutants on the Risk of MI

Figure 3 presents the effect of each one-unit increase in air pollutants on MI risk across different lag periods. For the single-day lag effect, the impacts of air pollutants on MI risk generally showed a decreasing trend as the number of lag days increased. The effects of PM_{2.5}, PM₁₀, SO₂, NO₂, and CO were no longer significant after 5 days of exposure. In terms of the cumulative lag effect, with the increase in cumulative lag days, PM_{2.5}, PM₁₀, SO₂, NO₂, and CO all exhibited a trend of first increasing and then decreasing, reaching the peak at lag 05. At lag 05, each one-unit increase in air pollutants was associated with a respective increase in MI risk of 0.57% (0.38%, 0.76%), 0.56% (0.43%, 0.69%), 4.50% (3.32%, 5.70%), 3.59% (3.03%, 4.15%), and 10.32% (8.25%, 12.42%). In contrast, O₃ exhibited a consistent decreasing trend, with the strongest effect observed at lag 0 [0.37% (0.26%, 0.49%)].

At lag 05, critical thresholds were identified for PM_{2.5}, PM₁₀, SO₂, and CO. Before these critical thresholds, no significant associations with MI risk were observed; however, beyond the thresholds, each one-unit increase in air pollutant concentrations was associated with respective increases in MI risk of 0.63% (0.45%, 0.82%), 2.78% (2.06%, 3.50%), 5.31% (3.82%, 6.83%), and 16.11% (12.83%, 19.48%). Each 10 µg/m³ increase in NO₂ concentration was associated with a 3.59% (3.03%, 4.15%) increase in MI risk, with no obvious linear deviation observed. At lag 0, for O₃, when its concentration was less than 77.08 µg/m³, each 10 µg/m³ increase was associated with a 7.13% (5.55%, 8.68%) decrease in MI risk; in contrast, when O₃ concentration exceeded 77.08 µg/m³, each 10 µg/m³ increase was associated with a 0.37% (0.24%, 0.51%) increase in MI risk (Fig. 4; Table 2).

Interactions of temperature variations and air pollution on the risk of MI

Interactive effects of air pollution and high DTR on the risk of MI were further explored using three interaction metrics: REOI, AP, and SI (Table 3; Tables S2–S6). The results revealed significant interactive effects between various air pollutants and high DTR across multiple lag periods. For instance, at lag 2, the REOI values for the interactions of PM_{2.5}, PM₁₀, SO₂, NO₂, and CO with high DTR were −0.0437 (−0.0662, −0.0213), −0.0575 (−0.0773, −0.0376), −0.0263 (−0.0465, −0.0062), −0.0547 (−0.0749, −0.0345), and −0.0302 (−0.0497, −0.0106), respectively. These findings indicated an antagonistic interaction between the aforementioned air pollutants and high DTR. At lag 07, the REOI, AP, and SI for the interaction between O₃ and high DTR were −0.0208 (−0.0411, −0.0004), −0.0208 (−0.0412, −0.0004), and −0.1130 (−0.1277, 0.9015), respectively, confirming an antagonistic interaction between O₃ and high DTR as well.

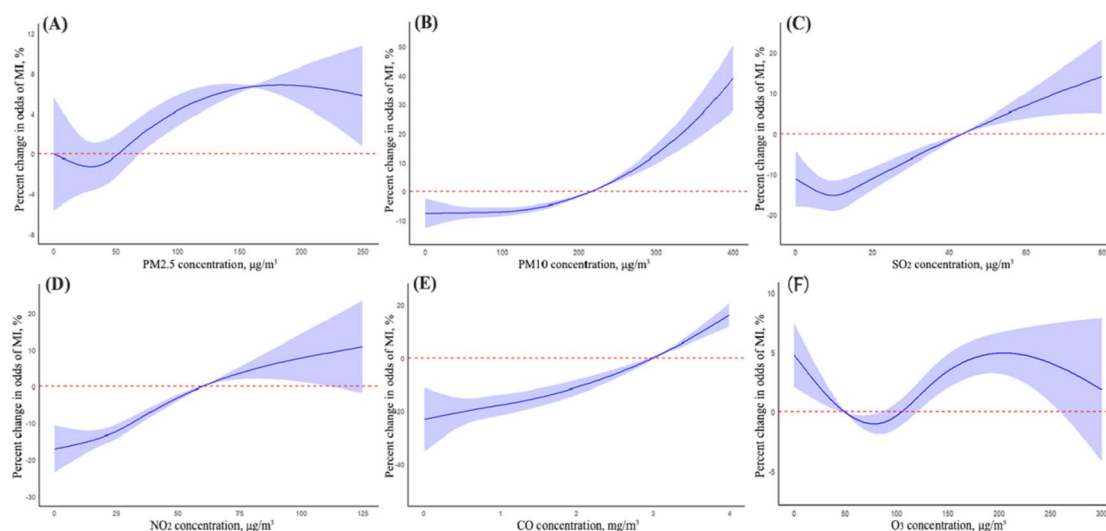


Fig. 4. Exposure-response association of short-term exposure to PM_{2.5}, PM₁₀, SO₂, NO₂, CO, and O₃ during their respective periods of strongest effect and the risk of MI. The solid blue lines with shaded regions indicated percent changes in odds of MI risk and their corresponding 95% CI, respectively. The red dotted lines represented the referent percent change of 0.

	Breakpoint	Percent Change (95% CI)		P nonlinear
		< Breakpoint	> Breakpoint	
PM _{2.5}	24.87 µg/m ³	-4.86 (-11.17, 1.89)	0.63 (0.45, 0.82)	<0.001
PM ₁₀	179.97 µg/m ³	0.13 (-0.06, 0.31)	2.78 (2.06, 3.50)	<0.001
SO ₂	14.02 µg/m ³	-0.21 (-3.41, 3.09)	5.31 (3.82, 6.83)	<0.001
CO	1.28 mg/m ³	1.01 (-3.63, 5.88)	16.11 (12.83, 19.48)	<0.001
O ₃	77.08 µg/m ³	-7.13 (-8.68, -5.55)	0.37 (0.24, 0.51)	<0.001

Table 2. Estimated percent change in odds of MI risk associated with exposure to each 1-unit increase in air pollutants. *MI* myocardial infarction, *PM_{2.5}* fine particulate matter, *PM₁₀* inhalable particulate matter, *NO₂* nitrogen dioxide, *CO* carbon monoxide, *O₃* ozone.

Stratified analysis

Females exhibited significantly greater susceptibility to MI associated with SO₂ and NO₂ exposure compared with males. Moreover, the independent effects of SO₂ and NO₂ on MI risk were more pronounced among individuals aged ≥ 65 years than among those aged < 65 years ($P_{\text{difference}} < 0.05$). The effects of PM_{2.5} and PM₁₀ on MI were significantly stronger in the warm season than in the cold season, whereas CO showed a more prominent effect during the cold season.

High DTR was significantly associated with an increased risk of MI among individuals aged ≥ 65 years. Compared with males, females were more susceptible to high DTR-related MI. Notably, the protective effect of low DTR was more evident in individuals aged < 65 years and was also significantly stronger in the warm season than in the cold season.

Regarding interaction effects, antagonistic interactions between air pollutants and high DTR were observed in specific subgroups. Among males, exposure to PM_{2.5}, SO₂, or NO₂ showed antagonistic interactions with high DTR. Similarly, among individuals aged ≥ 65 years, exposure to SO₂ and NO₂ also demonstrated antagonistic interactions with high DTR. In seasonal analyses, SO₂ exhibited a significant antagonistic interaction with high DTR in the warm season, whereas NO₂ showed a significant antagonistic interaction with high DTR in the cold season. However, after stratification by sex or age, the differences in interaction effects were not statistically significant ($P_{\text{difference}} < 0.05$; Table 4, S7 and S8).

Sensitivity analysis

Sensitivity analysis was performed by excluding patients with subsequent MI (ICD-10 code I22) to validate the robustness of these findings. The results showed that the antagonistic effects observed in the interaction between air pollution and high DTR were consistent with those from the primary analysis (Table S9). All other significant associations identified in the initial analysis remained statistically significant (Figure S1).

To eliminate the impact of coronavirus disease 2019 (COVID-19), we restricted the patients' onset time to the period from 2017 to 2019. The results showed that all six air pollutants and high DTR significantly increased the risk of MI, which was consistent with the findings of the main analysis. Significant antagonistic effects were

PM2.5	Estimate (95% CI)		
	REOI	AP	SI
lag0	-0.0370 (-0.0598, -0.0142)	-0.0359 (-0.0582, -0.0136)	0.4480 (0.2117, 0.6842)
lag1	-0.0209 (-0.0439, 0.0020)	-0.0198 (-0.0417, 0.0020)	0.7252 (0.4827, 0.9678)
lag2	-0.0437 (-0.0662, -0.0213)	-0.0439 (-0.0665, -0.0212)	-0.0775 (-0.5638, 0.4087)
lag3	-0.0672 (-0.0897, -0.0447)	-0.0679 (-0.0908, -0.0450)	-0.1716 (-0.5452, 0.2019)
lag4	-0.0075 (-0.0297, 0.0145)	-0.0074 (-0.0293, 0.0143)	0.6584 (-0.1025, 1.4194)
lag5	-0.0122 (-0.0345, 0.0101)	-0.0119 (-0.0338, 0.0099)	0.6436 (0.1516, 1.1356)
lag6	-0.0167 (-0.0392, 0.0058)	-0.0162 (-0.0382, 0.0057)	0.6153 (0.2298, 1.0008)
lag7	-0.0321 (-0.0548, -0.0095)	-0.0314 (-0.0537, -0.0092)	0.4055 (0.1149, 0.6960)
lag01	-0.0314 (-0.0545, -0.0082)	-0.0300 (-0.0522, -0.0078)	0.5943 (0.3744, 0.8142)
lag02	-0.0216 (-0.0445, 0.0013)	-0.0208 (-0.0429, 0.0013)	0.6363 (0.3461, 0.9264)
lag03	-0.0096 (-0.0323, 0.0129)	-0.0093 (-0.0312, 0.0125)	0.7832 (0.3619, 1.2044)
lag04	0.0052 (-0.0174, 0.0278)	0.0049 (-0.0164, 0.0263)	1.0997 (0.6291, 1.5703)
lag05	0.0335 (0.0113, 0.0557)	0.0317 (0.0107, 0.0527)	2.5310 (-0.2761, 5.3382)
lag06	0.0483 (0.0260, 0.0706)	0.0451 (0.0244, 0.0659)	3.1893 (-0.4579, 6.8366)
lag07	0.0596 (0.0372, 0.0821)	0.0557 (0.0349, 0.0766)	6.6415 (-10.5185, 23.8016)

Table 3. Interactions of high DTR and PM2.5 on MI risk. *MI* myocardial infarction, *DTR* diurnal temperature range, *REOI* relative excess odds due to interaction, *AP* attributable proportion of interaction, *SI* synergy index, *PM2.5* fine particulate matter.

Subgroups	Pollutants	Estimate value (95% CI)		
		REOI	AP	SI
Male	PM2.5	-0.0437 (-0.0701, -0.0172)	-0.0420 (-0.0676, -0.0164)	0.4734 (0.2490, 0.6977)
	PM10	0.0097 (-0.0163, 0.0357)	0.0094 (-0.0157, 0.0344)	1.3489 (0.0766, 2.6212)
	SO ₂	-0.0580 (-0.0858, -0.0303)	-0.0562 (-0.0831, -0.0292)	0.3637 (0.1776, 0.5499)
	NO ₂	-0.0671 (-0.0941, -0.0401)	-0.0660 (-0.0927, -0.0393)	0.1963 (-0.0254, 0.4180)
	CO	-0.0164 (-0.0431, 0.0103)	-0.0157 (-0.0414, 0.0100)	0.7245 (0.3511, 1.0978)
	O ₃	0.0529 (0.0265, 0.0793)	0.0510 (0.0256, 0.0763)	-2.6611 (-10.3806, 5.0585)
Female	PM2.5	-0.0060 (-0.0369, 0.0249)	-0.0057 (-0.0351, 0.0237)	0.8958 (0.04049, 1.3866)
	PM10	0.0407 (0.0104, 0.0710)	0.0388 (0.0100, 0.0677)	6.6260 (-25.8070, 39.0590)
	SO ₂	-0.0271 (-0.0594, 0.0051)	-0.0261 (-0.0572, 0.0050)	0.5873 (0.2522, 0.9224)
	NO ₂	0.0056 (-0.0253, 0.0365)	0.0054 (-0.0244, 0.0352)	1.1801 (0.0111, 2.3492)
	CO	-0.0231 (-0.0547, 0.0084)	-0.0220 (-0.0523, 0.0082)	0.6788 (0.3220, 1.0256)
	O ₃	0.0217 (-0.0102, 0.0535)	0.0205 (-0.0096, 0.0506)	1.5859 (0.1684, 3.0034)
<65y	PM2.5	-0.0287 (-0.0603, 0.0030)	-0.0279 (-0.0588, 0.0030)	0.4829 (0.0820, 0.8838)
	PM10	-0.0110 (-0.0424, 0.0205)	-0.0108 (-0.0419, 0.0203)	0.5282 (-0.3510, 1.4073)
	SO ₂	-0.0291 (-0.0619, 0.0036)	-0.0293 (-0.0622, 0.0037)	-0.1444 (-1.2245, 0.9356)
	NO ₂	-0.0308 (-0.0625, 0.0010)	-0.0312 (-0.0634, 0.0011)	-0.6633 (-3.1131, 1.7865)
	CO	-0.0246 (-0.0566, 0.0073)	-0.0243 (-0.0560, 0.0074)	0.3531 (-0.2988, 1.0050)
	O ₃	0.0299 (-0.0022, 0.0619)	0.0292 (-0.0021, 0.0604)	-4.0716 (-37.2268, 29.0836)
≥ 65y	PM2.5	-0.0221 (-0.0481, 0.0038)	-0.0210 (-0.0457, 0.0037)	0.7119 (0.4445, 0.9792)
	PM10	0.0492 (0.0240, 0.0744)	0.0464 (0.0227, 0.0702)	5.9205 (-11.3623, 23.2033)
	SO ₂	-0.0498 (-0.0771, -0.0225)	-0.0470 (-0.0728, -0.0212)	0.5469 (0.3814, 0.7124)
	NO ₂	-0.0291 (-0.0553, -0.0028)	-0.0277 (-0.0529, -0.0026)	0.6195 (0.3686, 0.8705)
	CO	-0.0138 (-0.0403, 0.0127)	-0.0129 (-0.0377, 0.0120)	0.8381 (0.5596, 1.1166)
	O ₃	0.0472 (0.0208, 0.0735)	0.0442 (0.0196, 0.0689)	3.4688 (-2.1011, 9.0386)

Table 4. Interactions of high DTR and air pollution on MI risk by subgroup analysis. *MI* myocardial infarction, *DTR* diurnal temperature range, *REOI* relative excess odds due to interaction, *AP* attributable proportion of interaction, *SI* synergy index, *PM2.5* fine particulate matter, *PM10* inhalable particulate matter, *SO₂* sulfur dioxide, *NO₂* nitrogen dioxide, *CO* carbon monoxide, *O₃* ozone.

observed between exposures to SO₂, NO₂ and high DTR on the risk of acute MI; no significant interactions were found between the remaining air pollutants and high DTR exposure, which was generally consistent with the results of the main analysis (Table S10 and Figure S2).

Discussion

This study represented case-crossover analysis based on individual exposure to investigate interactive effect of DTR and air pollution on MI incidence. By analyzing data from 391,901 MI patients across a central Chinese province during 2017–2020, we demonstrated that short-term exposure to air pollutants and high DTR significantly elevated MI risk. Notably, antagonistic effects were observed between air pollutants and high DTR, which indicated that combined exposure may mitigate MI risk. Our findings further revealed that SO₂ and NO₂ exert stronger impacts on female patients and individuals aged ≥65 years old, who also exhibited heightened susceptibility to diurnal temperature fluctuations.

To date, few studies have investigated the association between DTR and MI morbidity, with most research focusing on MI mortality^{23,24}. Consequently, the impact of DTR on MI risk remains unclear. Lee et al.'s findings indicated that beyond threshold temperatures (spring: 7.5 °C, winter: 6.5 °C), each 1 °C increase in DTR elevated the risk of MI emergency visits by 3.0% and 2.0% in spring and winter, respectively²⁵. However, a Korean case-crossover study reported no significant association between DTR and MI admission rates¹¹. In contrast, our study observed that every 1 °C increase in high DTR (> 13.5 °C) raised MI risk by 0.67%, while low DTR exerted a protective effect on the population. These discrepancies may stem from regional and population differences, as South Korea's average DTR during its study period (8 °C, SD = 3 °C) was lower than our study (10.5 °C, SD = 3.7 °C). Our study confirmed that the elderly heightened vulnerability to DTR, consistent with most prior research²⁶. At the same time, this study observed a protective association between low DTR and MI incidence. Lower diurnal variability reflects a more thermally stable environment, which may reduce acute thermoregulatory stress and sympathetic nervous system activation. Such temperature stability could attenuate fluctuations in blood pressure, vascular tone, and blood viscosity—pathways known to contribute to the triggering of acute coronary events^{27,28}.

Over recent decades, most research have focused on associations between short-term air pollution exposure and MI mortality^{29,30}, while studies examining MI incidence remain relatively scarce. Our findings demonstrated that MI risk increased significantly with rising exposure to PM_{2.5}, PM₁₀, SO₂, and CO, with the presence of threshold effects. This aligns with a large Chinese case-control study reported that each interquartile range increase in acute exposure to PM_{2.5}, SO₂, and CO elevated MI risk by 1.32%, 0.67%, and 1.55% respectively, with threshold effects also observed³¹. An Italian study confirmed positive overall correlations between PM₁₀, SO₂, CO and MI incidence, but did not account for nonlinear associations, potentially underestimating effects at lower exposure levels^{32,33}. Regarding O₃, a Chinese study found no significant association with MI incidence³¹, contrasting with a U.S. case-crossover study that reported significant effects from short-term O₃ exposure³⁴. Our analysis revealed an inverse relationship with MI risk below 77.08 µg/m³ of O₃, but a significant increase beyond this threshold, indicated divergent findings across studies that warrant deeper investigation. A meta-analysis indicated that each 10 µg/m³ increase in short-term NO₂ exposure was significantly associated with a 1.0% elevation in MI incidence³⁵. In our study, every 10 µg/m³ increment in NO₂ concentration increased MI risk by 3.59%, with both studies demonstrating consistent findings. Against the backdrop of increasingly complex climate change, both large temperature variations and air pollution events are occurring with greater frequency. Consequently, investigating their combined effects has become critically important. Our findings revealed antagonistic effects between air pollutants with high DTR, where co-exposure actually reduced MI risk. On the one hand, when large DTR coincide with severe air pollution, individuals may proactively adopt protective measures, reduced outdoor activity and adjusted clothing promptly, and mitigated health risks. In contrast, when large temperature variations or air pollution occur in isolation, preventive awareness may wane, increasing vulnerability to individual exposures³⁶. On the other hand, a large diurnal temperature range reflects greater intraday temperature variability. Such variability may influence atmospheric dispersion conditions and human physiological responses, thereby potentially modifying the health effects of air pollutants. Although the co-exposure to high DTR and air pollution exhibited antagonistic effects, this interaction does not imply that large temperature variations or severe pollution confer health benefits. Instead, such adverse weather conditions may prompt heightened self-protection behaviors, which could buffer health impacts. On the premise of improving air quality, timely issuance of large DTR warnings is essential to safeguard public health.

This study offered several key strengths. Firstly, it represented the inaugural investigation into the combined impact of DTR and air pollution on MI incidence risk. Secondly, leveraging a population base of 99.36 million in Henan Province, the inclusion of 391,901 MI patients provided substantial statistical power for robustly examining these associations. Thirdly, the application of a time-stratified case-crossover design inherently controls for personal confounders (e.g., age, gender, socioeconomic status, lifestyle) as well as long-term trends and seasonality by using each case as its own control. Finally, individual exposure assessment based on residential addresses at symptom onset enhances the accuracy of assigned air pollution and temperature exposure estimates. Notably, several limitations should be acknowledged. Firstly, while pollution and meteorological data were matched to patients' residential addresses, the absence of individual indoor exposure data introduces inevitable potential for exposure misclassification. Secondly, these findings from this central Chinese province require caution when generalizing to other regions, though they provided valuable references for similar geographical contexts.

Conclusions

This study demonstrated that exposure to PM_{2.5}, PM₁₀, SO₂, NO₂, CO, and O₃ significantly elevates the risk of MI onset. Notably, non-linear associations were identified between PM_{2.5}, PM₁₀, SO₂, CO, O₃, and the development of MI. High DTR was significantly linked to MI, particularly affecting women and older adults as susceptible populations. Additionally, antagonistic effects were observed between air pollutants and high DTR exposure, which indicated that high DTR may mitigate the adverse effects of air pollutants on MI risk. These findings underscore the imperative to enhance early warnings for extreme thermal variations alongside air pollution mitigation, prompting individuals to implement timely preventive measures for health protection.

Data availability

The air pollution and meteorological datasets used in this study were obtained from the following public domain resources: <https://data.tpdc.ac.cn> and <https://www.ecmwf.int>.

Received: 11 December 2025; Accepted: 24 March 2026

Published online: 29 March 2026

References

- Hansel, N. N., McCormack, M. C. & Kim, V. The Effects of Air Pollution and Temperature on COPD. *Copd* <https://doi.org/10.3109/15412555.2015.1089846> (2016).
- IPCC. Climate Change 2021: The Physical Science Basis. (2021). <https://www.ipcc.ch/report/ar6/wg1/>
- Alahmad, B. et al. Associations Between Extreme Temperatures and Cardiovascular Cause-Specific Mortality: Results From 27 Countries. *Circulation* <https://doi.org/10.1161/CIRCULATIONAHA.122.061832> (2023).
- Faurie, C. et al. Association between high temperature and heatwaves with heat-related illnesses: A systematic review and meta-analysis. *Sci Total Environ* <https://doi.org/10.1016/j.scitotenv.2022.158332> (2022).
- Tran, H. M. et al. Extreme temperature increases the risk of COPD morbimortality: A systematic review and meta-analysis. *Sci Total Environ* <https://doi.org/10.1016/j.scitotenv.2024.178087> (2025).
- Pan, R. et al. Association between ambient temperature and cause-specific cardiovascular disease admissions in Japan: A nationwide study. *Environ Res* <https://doi.org/10.1016/j.envres.2023.115610> (2023).
- Wang, B. et al. Association between ambient temperature and cardiovascular disease hospitalisations among farmers in suburban northwest China. *Int J Biometeorol* <https://doi.org/10.1007/s00484-022-02278-2> (2022).
- Wang, X. et al. Impact of temperature variability on childhood allergic rhinitis in a subtropical city of China. *BMC Public Health* <https://doi.org/10.1186/s12889-020-09531-6> (2020).
- Zhang, F. et al. Ambient temperature variations and AIDS-related mortality: A time-stratified case-crossover study in 103 counties, China. *Sci Total Environ* <https://doi.org/10.1016/j.scitotenv.2023.169474> (2024).
- Sharafkhani, R. et al. Diurnal temperature range and mortality in Urmia, the Northwest of Iran. *J Therm Biol* <https://doi.org/10.1016/j.jtherbio.2017.08.011> (2017).
- Lim, Y. H., Hong, Y. C. & Kim, H. Effects of diurnal temperature range on cardiovascular and respiratory hospital admissions in Korea. *Sci Total Environ* <https://doi.org/10.1016/j.scitotenv.2011.12.048> (2012).
- Xu, D. et al. Triglyceride-rich lipoproteins and cardiovascular diseases. *Front Endocrinol (Lausanne)* <https://doi.org/10.3389/fendo.2024.1409653> (2024).
- Hoole, S. P. & Bambrough, P. Recent advances in percutaneous coronary intervention. *Heart* <https://doi.org/10.1136/heartjnl-2019-315707> (2020).
- Benjamin, E. J. et al. Heart disease and stroke statistics-2019 update: A report from the American Heart Association. *Circulation* **96**, e56–e528 (2019).
- Cohen, A. J. et al. Estimates and 25-year trends of the global burden of disease attributable to ambient air pollution: an analysis of data from the Global Burden of Diseases Study 2015. *Lancet* [https://doi.org/10.1016/S0140-6736\(17\)30505-6](https://doi.org/10.1016/S0140-6736(17)30505-6) (2017).
- de Bont, J. et al. Ambient air pollution and cardiovascular diseases: An umbrella review of systematic reviews and meta-analyses. *J Intern Med* <https://doi.org/10.1111/joim.13467> (2022).
- Xu, R. et al. Extreme Temperature Events, Fine Particulate Matter, and Myocardial Infarction Mortality. *Circulation* <https://doi.org/10.1161/CIRCULATIONAHA.122.063504> (2023).
- Wei, J. & Li, Z. ChinaHighPM2.5: High-resolution and High-quality Ground-level PM_{2.5} Dataset for China (2000–2023). National Tibetan Plateau Data Center. (2024). <https://doi.org/10.5281/zenodo.3539349>
- Janes, H., Sheppard, L. & Lumley, T. Case-crossover analyses of air pollution exposure data: referent selection strategies and their implications for bias. *Epidemiology* <https://doi.org/10.1097/01.ede.0000181315.18836.9d> (2005).
- Li, M. et al. Air pollution and stroke hospitalization in the Beibu Gulf Region of China: A case-crossover analysis. *Ecotoxicol Environ Saf* <https://doi.org/10.1016/j.ecoenv.2023.114814> (2023).
- Xu, R. et al. Ozone, Heat Wave, and Cardiovascular Disease Mortality: A Population-Based Case-Crossover Study. *Environ Sci Technol* <https://doi.org/10.1021/acs.est.3c06889> (2024).
- Knol, M. J. & VanderWeele, T. J. Recommendations for presenting analyses of effect modification and interaction. *Int J Epidemiol* <https://doi.org/10.1093/ije/dyr218> (2012).
- Gu, X. et al. The synergy between diurnal temperature range and calcium concentration help to predict hospital mortality in patients with acute myocardial infarction. *Sci Rep* <https://doi.org/10.1038/s41598-022-18816-2> (2022).
- Song, Z. Y. et al. [Analysis of the association between diurnal temperature difference and relative humidity and myocardial infarction in Shantou residents]. *Zhonghua Liu Xing Bing Xue Za Zhi*, 1622–1627. (2023).
- Lee, S. et al. Short-term effect of temperature on daily emergency visits for acute myocardial infarction with threshold temperatures. *PLoS One* <https://doi.org/10.1371/journal.pone.0094070> (2014).
- Tang, H. et al. Long-Term Impacts of Diurnal Temperature Range on Mortality and Cardiovascular Disease: A Nationwide Prospective Cohort Study. *Metabolites* <https://doi.org/10.3390/metabo12121287> (2022).
- Bhaskaran, K. et al. Effects of ambient temperature on the incidence of myocardial infarction. *Heart* <https://doi.org/10.1136/hrt.2009.175000> (2009).
- Cheng, J. et al. Impact of diurnal temperature range on human health: a systematic review. *Int J Biometeorol* <https://doi.org/10.1007/s00484-014-0797-5> (2014).
- Liu, Y. et al. Short-Term Exposure to Ambient Air Pollution and Mortality From Myocardial Infarction. *J Am Coll Cardiol* <https://doi.org/10.1016/j.jacc.2020.11.033> (2021).
- Miri, M. et al. Mortality and morbidity due to exposure to outdoor air pollution in Mashhad metropolis, Iran. The AirQ model approach. *Environ Res* <https://doi.org/10.1016/j.envres.2016.07.039> (2016).
- Chen, R. et al. Hourly Air Pollutants and Acute Coronary Syndrome Onset in 1.29 Million Patients. *Circulation* <https://doi.org/10.1161/CIRCULATIONAHA.121.057179> (2022).

32. Nuvolone, D. et al. Short-term association between ambient air pollution and risk of hospitalization for acute myocardial infarction: results of the cardiovascular risk and air pollution in Tuscany (RISCAT) study. *Am J Epidemiol* <https://doi.org/10.1093/aje/kwr046> (2011).
33. Chen, C. et al. Short-term exposures to PM(2.5) and cause-specific mortality of cardiovascular health in China. *Environ Res* <https://doi.org/10.1016/j.envres.2017.10.046> (2018).
34. Zhang, S. et al. Short-Term Associations Between Ambient Ozone and Acute Myocardial Infarction Onset Among Younger Patients: Results From the VIRGO Study. *Geohealth* <https://doi.org/10.1029/2024GH001234> (2025).
35. Mustafic, H. et al. Main air pollutants and myocardial infarction: a systematic review and meta-analysis. *Jama* <https://doi.org/10.1001/jama.2012.126> (2012).
36. Cheng, C. et al. Effects of extreme temperature events on deaths and its interaction with air pollution. *Sci Total Environ* <https://doi.org/10.1016/j.scitotenv.2024.170212> (2024).

Author contributions

Xi-yun Gong: Data Curation, Visualization, Writing - original draft. Zai-chao Dong: Data Curation, Visualization, Writing - original draft. Tong-tong Sha and Qian Li: Investigation, Visualization, Data curation. Yan-jie Dou and Huan-xia Zhang: Investigation, Data curation. Yao Li: Visualization. Hai-tao Wei and Fang-fang Yu: Funding acquisition, Conceptualization, Writing - review & editing. All authors read and approved the final manuscript.

Funding

This research was funded by Key R&D Special Project of Henan Province (261111212800), Henan Province Natural Science Foundation (252300423223).

Declarations

Competing interests

The authors declare no competing interests.

Ethics approval and consent to participate

Not applicable (Our manuscript does not report or involve the use of any animal or human data or organisations.)

Consent for publication

Not applicable (Our manuscript does not contain data from any individual person.)

Ethical statement

The study protocol was carried out in accordance with relevant guidelines and regulations. The study protocol was approved by the Ethics Committee of Zhengzhou University.

Informed consent

The study protocol was informed consent was obtained from all subjects and/or their legal guardians.

Additional information

Supplementary Information The online version contains supplementary material available at <https://doi.org/10.1038/s41598-026-46261-y>.

Correspondence and requests for materials should be addressed to H.-t.W. or F.-f.Y.

Reprints and permissions information is available at www.nature.com/reprints.

Publisher's note Springer Nature remains neutral with regard to jurisdictional claims in published maps and institutional affiliations.

Open Access This article is licensed under a Creative Commons Attribution-NonCommercial-NoDerivatives 4.0 International License, which permits any non-commercial use, sharing, distribution and reproduction in any medium or format, as long as you give appropriate credit to the original author(s) and the source, provide a link to the Creative Commons licence, and indicate if you modified the licensed material. You do not have permission under this licence to share adapted material derived from this article or parts of it. The images or other third party material in this article are included in the article's Creative Commons licence, unless indicated otherwise in a credit line to the material. If material is not included in the article's Creative Commons licence and your intended use is not permitted by statutory regulation or exceeds the permitted use, you will need to obtain permission directly from the copyright holder. To view a copy of this licence, visit <http://creativecommons.org/licenses/by-nc-nd/4.0/>.

© The Author(s) 2026